



Fermi National Accelerator Laboratory

FERMILAB-Pub-90/19-T

February 1, 1990

**The coupling of the QCD pomeron in various semihard processes**

**R. K. Ellis**

*Fermi National Accelerator Laboratory  
P.O. Box 500, Batavia, Illinois 60510, U.S.A.*

*and*

**D. A. Ross**

*Department of Physics, University of Southampton  
Southampton SO9 5NH, U.K.*

**Abstract**

The higher order contributions to various QCD processes are considered. The terms due to the exchange of an eikonal gluon between the incoming partons are studied. These terms dominate the high energy behaviour. This allows the extraction of the impact factor for each of these processes and hence the strength of their lowest order couplings to the QCD pomeron. After examination of the relationship between the parts that are dependent and independent of the subtraction point in the  $\overline{MS}$  scheme, an alternative subtraction scheme is proposed in which most of the large correction arising in this kinematical region is absorbed into the gluon distribution function.



## 1. Introduction

There has recently been a great deal of interest in signals for pomeron exchange in perturbative QCD[1,2]. The picture of the pomeron which emerges is the sum of all graphs involving the exchange of two low  $q^2$  gluons joined together by other gluons forming crossed and uncrossed ladders. If  $q^2$  is sufficiently large, the methods of perturbative QCD are applicable. The sum of these graphs is referred to as the perturbative pomeron. This pomeron dominates the forward scattering amplitude of two gluons. In particular, the imaginary part of the pomeron exchange is the cross section for some process in which a single eikonal gluon is exchanged and that gluon emits further gluons which manifest themselves as minijets. These minijets have been shown in ref. [3] to give rise to a shift in the intercept of the pomeron away from  $\alpha(0) = 1$ . To leading order we omit the minijets and consider the exchange of a single eikonal gluon. If one considers two jet production in hadron-hadron scattering, this exchange is present already in the lowest order contribution.

Many other hard processes occur in lowest order without such an exchange. Gluon exchange in the  $t$  channel is part of the higher order correction to such hard scattering processes. For large values of  $s$  this gluon exchange in the  $t$ -channel is the dominant part of the higher order contribution (at least at the parton level). This term is the most important at high energies since, unlike the leading order expression, it does not fall off like  $1/s$ . The dimensions of the cross-section are carried by some other quantity, such as the transverse momentum or heavy quark mass, which remains fixed as  $s$  becomes large. It is this  $s$  independence which permits the interpretation as pomeron exchange, leading to a parton cross section  $\hat{\sigma}$  which is constant in  $s$  (up to minijet corrections). In this paper we ignore the minijet corrections. However we present our results in such a way that we believe that they will be useful as first steps in the calculation of even higher order terms.

We consider the QCD corrections to three processes and show that the leading power piece has always approximately the same form. In calculating the contribution from eikonal gluon exchange and integrating over the phase space of the outgoing partons, one encounters a collinear divergence when the exchanged gluon goes on its mass shell. This collinear divergence is subtracted in the normal fashion[4] and absorbed into the parton distribution functions. Thus the perturbatively calculated

cross section  $\sigma$  for a process initiated by partons of type  $i$  and  $j$  may be written as,

$$\sigma_{ij}(s, m^2) = \sum_{i'j'} \int dx_1 dx_2 \hat{\sigma}_{i'j'}(x_1 x_2 s, m^2) \Gamma_{i'i}(x_1, \epsilon) \Gamma_{j'j}(x_2, \epsilon) \quad (1.1)$$

The short distance cross section  $\hat{\sigma}$  is free from collinear singularities and is calculable as a perturbation series in the running coupling constant. The collinear singularities have been regulated by continuation of the dimension of space time to  $n = 4 - 2\epsilon$  dimensions. For example, in the  $\overline{MS}$  factorisation scheme[5] the factorisation piece  $\Gamma$  is,

$$\Gamma_{ij}(x, \epsilon) = \left[ \delta_{ij} \delta(1-x) - \frac{1}{\epsilon} \frac{\alpha_S}{2\pi} P_{ij}(x) + O(\alpha_S^2) \right] \quad (1.2)$$

where

$$\frac{1}{\epsilon} = \frac{1}{\epsilon} + \ln 4\pi - \gamma_E. \quad (1.3)$$

$P_{ij}$  is the normal Altarelli-Parisi function[6] and  $\gamma_E$  is the Euler constant. For a process with an observed massless parton in the final state,  $p_1 + p_2 \rightarrow p_3 + X$ , the factorisation formula becomes,

$$\frac{E_3 d\sigma_{ij}^k}{d^{n-1}p_3} = \sum_{i'j'k'} \int dx_1 dx_2 \frac{dx_3}{x_3^2} \Gamma_{kk'}(x_3, \epsilon) \frac{\hat{E}_3 d\hat{\sigma}_{i'j'}^k}{d^{n-1}\hat{p}_3} \Gamma_{i'i}(x_1, \epsilon) \Gamma_{j'j}(x_2, \epsilon) \quad (1.4)$$

The short distance cross section  $\hat{\sigma}$  is evaluated at rescaled values of the parton momenta,  $\hat{p}_1 = x_1 p_1$ ,  $\hat{p}_2 = x_2 p_2$ ,  $\hat{p}_3 = p_3/x_3$ .

The finite parts of the factorisation piece,  $\Gamma$ , are subject to a prescription ambiguity. One has the freedom to subtract any finite part along with the collinear divergence. At high energy we find that most of the leading power higher order corrections to the processes considered here can be removed by a suitable choice of this finite part. What this means, in effect, is that factorisation prescription dependence allows one to reduce considerably the coupling of the perturbative pomeron to these hard scattering processes. This leads to a gluon distribution which is different from the distribution defined in the  $\overline{MS}$  factorisation scheme. Since the modification necessary to reduce the coupling to the QCD pomeron is proportional to  $1/x$ , the gluon distribution function is only affected at low  $x$ . We will discuss the effects of this alteration of the gluon distribution function in later sections.

## 2. High energy behaviour of heavy quark production

In this section we consider the high energy behaviour of the photoproduction and hadroproduction of heavy quarks. In perturbation theory the short distance cross section for the photoproduction of heavy quarks of mass  $m$  and electric charge  $e_Q$  may be written as,

$$\hat{\sigma}_{\gamma j} = \frac{e_Q^2 \alpha \alpha_S(\mu^2)}{m^2} \left\{ c_{\gamma j}^{(0)}(\rho) + 4\pi \alpha_S \left[ c_{\gamma j}^{(1)}(\rho) + \ln \left( \frac{\mu^2}{m^2} \right) \bar{c}_{\gamma j}^{(1)}(\rho) \right] + \dots \right\}. \quad (2.1)$$

The corresponding result for the hadroproduction of heavy quarks is,

$$\hat{\sigma}_{ij} = \frac{\alpha_S^2(\mu^2)}{m^2} \left\{ f_{ij}^{(0)}(\rho) + 4\pi \alpha_S \left[ f_{ij}^{(1)}(\rho) + \ln \left( \frac{\mu^2}{m^2} \right) \bar{f}_{ij}^{(1)}(\rho) \right] + \dots \right\} \quad (2.2)$$

where  $\rho = 4m^2/s$  and  $s$  is the square of the total parton-parton centre of mass energy. The labels  $i$  and  $j$  indicate the types of the incoming partons and  $\mu$  is the factorisation and renormalisation point. The diagrams which contribute in lowest order are shown in Fig. 1. The lowest order matrix elements squared obtained from these diagrams are given in Table 1. The notation  $\overline{\sum}$  indicates the average and sum over initial and final colours and spins. By convention, the average over incoming gluon and photon spins is performed assuming  $n - 2$  polarisations. The formulae are presented in  $n = 4 - 2\epsilon$  dimensions and the kinematic variables are

$$\tau_1 = \frac{p_1 \cdot p_3}{p_1 \cdot p_2}, \quad \tau_2 = \frac{p_2 \cdot p_3}{p_1 \cdot p_2}, \quad \rho = \frac{2m^2}{p_1 \cdot p_2}. \quad (2.3)$$

The expressions for the coefficients  $c^{(0)}$  and  $f^{(0)}$  which are obtained from the matrix elements in Table 1 are presented in Table 2. For gluon-quark scattering there is no leading order contribution to heavy quark production. Analytic expressions for the functions  $\bar{c}^{(1)}$  and  $\bar{f}^{(1)}$  can be found in refs. [7] and [8] respectively. Analytic expressions for the functions  $c^{(1)}$  and  $f^{(1)}$  are not available, although in refs. [7] and [8] a fit to numerical results is provided. Numerical results for  $c^{(1)}$  for the photon-gluon process as a function of  $\rho$  are shown in Fig. 2, taken from ref. [7]. The corresponding results for photon-gluon scattering are shown in Fig. 3 taken from ref. [8]. As can be seen the leading order contributions vanish in the high  $s$  limit, so for sufficiently large energies these parton cross sections are dominated by the higher order diagrams which

involve the exchange of a spin one gluon in the  $t$ -channel. In this section we describe the analytic calculation of these dominant contributions in perturbation theory.

We shall begin by studying the case of the photoproduction of heavy quarks. This problem has already been described in a somewhat different context in refs. [9,10]. Here we extend the calculation to give the results in  $n$ -dimensions. This is necessary to regulate the collinear divergences which are present when one uses a hard vertex to produce the exchanged eikonal gluon.

The general result for the diagrams with one gluon exchange in the  $t$ -channel can be written as,

$$\sigma = \frac{1}{2s} \int d^{(n)}PS_3 \overline{\sum} \left| \frac{U_\mu g^{\mu\lambda} L_\lambda}{q^2} \right|^2 \quad (2.4)$$

where  $U_\mu$  and  $L_\lambda$  are the upper and lower parts of the graph as shown in Fig 4.

The relevant diagrams and momentum assignments for the  $\gamma g$  process are shown in Fig. 5a. In the high energy limit the dominant contribution to the polarisation sum of the exchanged gluon is given by the replacement,

$$g^{\mu\lambda} \rightarrow \frac{2p_2^\mu p_1^\lambda}{s}, \quad s = 2p_1 \cdot p_2. \quad (2.5)$$

Following ref. [10] we perform a Sudakov decomposition of the momenta in the phase space integral.

$$\begin{aligned} p_3^\mu &= \alpha_3 p_1^\mu + \beta_3 p_2^\mu + t_3^\mu \\ q^\mu &= \alpha p_1^\mu + \beta p_2^\mu + q_T^\mu \end{aligned} \quad (2.6)$$

where  $p_1 \cdot q_T = p_2 \cdot q_T = p_1 \cdot t_3 = p_2 \cdot t_3 = 0$ . The dominant contribution to the cross-section at large  $s$  comes from the region  $\alpha \approx m^2/s, \beta \approx m^2/s$  and  $q^2 \approx -\vec{q}_T^2$ .

We shall define the function  $I$  in  $n$  dimensions as follows,

$$\begin{aligned} I &= \frac{1}{4\pi s} \frac{1}{(2\pi)^{n-2}} \int d(p_1 \cdot q) \int d^n p_3 d^n p_4 \delta(p_3^2 - m^2) \delta(p_4^2 - m^2) \delta^n(p_1 + q - p_3 - p_4) \\ &\quad \times \overline{\sum} \left[ \frac{p_2^\mu p_2^\nu}{p_1 \cdot p_2} U_\mu U_\nu^* \right]. \end{aligned} \quad (2.7)$$

$I$  describes the coupling of the eikonal gluon to the upper vertex at which the heavy quark pair is produced. It is closely related to the function known in the literature as

the impact factor[11]. In this paper we will refer to the function  $I$  defined by Eq. (2.7) as the impact factor. We further define the function  $K$  which describes the coupling of the incoming lower quark or gluon to the exchanged eikonal gluon,

$$K = \frac{1}{4\pi^2 s} \sum \left[ \frac{p_1^\lambda p_1^\rho}{p_1 \cdot p_2} L_\lambda L_\rho^* \right]. \quad (2.8)$$

With these definitions the result for the photoproduction cross section in the high energy limit may be written as,

$$\sigma_{ij} = \pi \frac{(4\pi)^\epsilon}{\Gamma(1-\epsilon)} \int \frac{d\vec{q}_T^2}{(\vec{q}_T^2)^{2+\epsilon}} \left[ \sum_{A,B} I_i^{AB} K_j^{AB} \right] + O\left(\frac{1}{s}\right). \quad (2.9)$$

The sums on  $A$  and  $B$  run over the colours of the exchanged gluons. The results for the functions  $K_i$  in the high energy limit are easily found to be,

$$K_q^{AB} = \frac{\alpha_S \mu^{2\epsilon}}{\pi} \frac{1}{N} \delta^{AB}, \quad K_g^{AB} = \frac{\alpha_S \mu^{2\epsilon}}{\pi} \frac{2N}{V} \delta^{AB}. \quad (2.10)$$

$N = 3$  is the number of colours of quarks and  $V = N^2 - 1$  is the number of colours of gluons. The scale  $\mu$  is introduced in Eq. (2.10) to keep the coupling constant dimensionless in  $n$  dimensions.

We now return to the calculation of the heavy quark photoproduction impact factor  $I_\gamma$ , as defined by Eq. (2.7). The calculation is performed using the Sudakov decomposition, Eq. (2.6), to define integration variables. The upper limit of the transverse momentum integral may be extended to infinity, if we neglect terms which are power suppressed at high energy. In this approximation we may combine denominators using a Feynman parameter  $x$  and shift the transverse momentum integral to obtain,

$$I_\gamma^{AB}(\vec{q}_T^2, m^2) = \frac{1}{2} \delta^{AB} \frac{e_Q^2 \alpha_S (4\pi \mu^4)^\epsilon}{\Gamma(2-\epsilon)} \int d\vec{t}^2 (t^2)^{-\epsilon} \int_0^1 d\alpha_3 A\left(\frac{\vec{q}_T^2}{m^2}, \alpha_3, t^2\right). \quad (2.11)$$

The function  $A$  is defined as follows

$$A\left(\frac{\vec{q}_T^2}{m^2}, \alpha_3, t^2\right) = \int_0^1 dx \left\{ \frac{\vec{q}_T^2 [1 - \epsilon - 2\alpha_3(1 - \alpha_3)(1 - 2x(1 - x))]}{[m^2 + x(1 - x)\vec{q}_T^2 + t^2]^2} - 4\alpha_3(1 - \alpha_3) \left[ \frac{m^2 + x(1 - x)\vec{q}_T^2}{[m^2 + x(1 - x)\vec{q}_T^2 + t^2]^2} - \frac{m^2}{[m^2 + t^2]^2} \right] \right\} \quad (2.12)$$

and  $\vec{t}$  is a Euclidean vector in the transverse space, ( $t^2 > 0$ ). Note that the function  $A$  vanishes for small  $\vec{q}_T^2$ . In the small  $\vec{q}_T$  limit it is given by,

$$A\left(\frac{\vec{q}_T^2}{m^2}, \alpha_3, \vec{t}^2\right) = \vec{q}_T^2 \int_0^1 dx \left\{ \frac{[1 - \epsilon - 2\alpha_3(1 - \alpha_3)]}{[m^2 + \vec{t}^2]^2} + \frac{8m^2 x(1-x)\alpha_3(1-\alpha_3)}{[m^2 + \vec{t}^2]^3} \right\} + O(\vec{q}_T^4) \quad (2.13)$$

The continuation to  $n$  dimensions is necessary to regulate the singularities present at  $\vec{q}_T = 0$  when the impact factor is inserted into a formula such as Eq. (2.9). It is therefore convenient to oversubtract the impact factor at  $\vec{q}_T = 0$  to make the singular terms manifest. We therefore introduce the four dimensional impact factor,  $\bar{I}_\gamma$ , which is the limit of Eq. (2.11) as  $n \rightarrow 4$ . For compactness of notation we express the four dimensional impact factor as follows,

$$\bar{I}_\gamma^{AB}(\vec{q}_T^2, m^2) = \delta^{AB} \frac{e_Q^2 \alpha_S}{2} h_\gamma\left(\frac{\vec{q}_T^2}{m^2}\right) \quad (2.14)$$

In terms of this function  $h_\gamma$  the result for the full photon impact factor may be written as,

$$I_\gamma^{AB}(\vec{q}_T^2, m^2) = \delta^{AB} \frac{e_Q^2 \alpha_S}{2} \left\{ \left[ h_\gamma\left(\frac{\vec{q}_T^2}{m^2}\right) - \frac{\vec{q}_T^2}{m^2} h'_\gamma(0) \theta(\mu^2 - \vec{q}_T^2) \right] + \theta(\mu^2 - \vec{q}_T^2) \frac{\vec{q}_T^2}{m^2} \frac{(4\pi\mu^2)^\epsilon}{\Gamma(2-\epsilon)} \left(\frac{\mu^2}{m^2}\right)^\epsilon \left(\frac{7}{9} - \frac{8}{9}\epsilon + O(\epsilon^2)\right) \right\} \quad (2.15)$$

The prime in the above equation indicates the derivative of the function  $h$  with respect to its argument. The explicit form for the function  $h_\gamma$  is given in Section 4. At this point the only property of  $h_\gamma$  which we require is the weighted integral,

$$\int_0^\infty \frac{da}{a^2} [h_\gamma(a) - a h'_\gamma(0) \theta(\mu^2 - am^2)] = \left[ \frac{41}{27} - \frac{7}{9} \ln\left(\frac{\mu^2}{m^2}\right) \right] \quad (2.16)$$

Inserting the full impact factor Eq. (2.15) in Eq. (2.9) we obtain the following result for the  $\gamma g$  cross-section.

$$\sigma_{\gamma g} = \frac{e_Q^2 \alpha_S^2}{m^2} \left\{ N \left[ \frac{41}{27} - \frac{7}{9} \ln\left(\frac{\mu^2}{m^2}\right) \right] + \frac{(4\pi\mu^2)^{2\epsilon}}{\Gamma(1-\epsilon)\Gamma(2-\epsilon)} \left(\frac{\mu^2}{m^2}\right)^\epsilon N \int_0^{\mu^2} \frac{d\vec{q}_T^2}{(\vec{q}_T^2)^{1+\epsilon}} \left(\frac{7}{9} - \frac{8}{9}\epsilon\right) \right\} \quad (2.17)$$

The short distance cross section is derived from the above result by factorising as given by Eq. (1.1). Only the branching on the leg with momentum  $p_2$  gives a leading contribution. From Eq. (1.1), the singular part of the cross-section is expected to be,

$$\sigma_{ij}^{\text{AP}} = -\frac{1}{\bar{\epsilon}} \frac{\alpha_S}{2\pi} \int dx_2 \hat{\sigma}_{ig}(p_1, x_2 p_2) P_{gj}(x_2), \quad \frac{1}{\bar{\epsilon}} = \frac{1}{\epsilon} + \ln 4\pi - \gamma_E \quad (2.18)$$

$\hat{\sigma}_{ig}$  is the total parton cross section calculated in  $n$  dimensions. In the high energy approximation the Altarelli-Parisi functions can be written as,

$$P_{gq}(z) = \frac{V}{Nz}, \quad P_{gg}(z) = \frac{2N}{z}. \quad (2.19)$$

Using the  $n$  dimensional result for the matrix element given in Table 1, we find that the end result for the  $\overline{MS}$  counterterms is,

$$\sigma_{\gamma g}^{\text{AP}} = \frac{e_Q^2 \alpha \alpha_S^2 (4\pi\mu^4)^\epsilon}{(m^2)^{1+\epsilon} \Gamma(2-\epsilon)} N \left[ -\frac{7}{9} \frac{1}{\bar{\epsilon}} + \frac{8}{9} \right]. \quad (2.20)$$

Subtracting Eq. (2.20) from Eq. (2.17) we obtain the final result for the short distance cross section for the photoproduction of a heavy quark,

$$\hat{\sigma}_{\gamma g} = \frac{e_Q^2 \alpha \alpha_S^2}{m^2} N \left[ \frac{41}{27} - \ln \left( \frac{\mu^2}{m^2} \right) \frac{7}{9} \right] + O\left(\frac{1}{s}\right) \quad (2.21)$$

Eq. (2.21) is in agreement with the results for  $c_{\gamma g}^{(1)}$ ,  $\bar{c}_{\gamma g}^{(1)}$  as defined in Eq. (2.1) and plotted in Fig. 2 in the high energy limit ( $\rho \rightarrow 0$ ). The corresponding result for the  $\gamma q$  process is simply related by a factor of  $V/(2N^2)$  expressing the relationship between  $K_g$  and  $K_q$  as shown in Eq. (2.10).

$$\hat{\sigma}_{\gamma q} = \frac{e_Q^2 \alpha \alpha_S^2}{m^2} \frac{V}{2N} \left[ \frac{41}{27} - \ln \left( \frac{\mu^2}{m^2} \right) \frac{7}{9} \right] + O\left(\frac{1}{s}\right) \quad (2.22)$$

We now turn to the calculation of the impact factor of the gluon which is slightly more complicated because of the presence of the three gluon coupling. The relevant diagrams are shown in Fig. 5b. The calculation proceeds in a similar way to the photoproduction calculation described above. The result for the impact factor of the gluon, as defined by Eq. (2.7), can be written in terms of the Sudakov variables as follows,

$$I_g^{AB}(\vec{q}_T^2, m^2) = \frac{1}{2V} \delta^{AB} \frac{\alpha_S^2 (4\pi\mu^4)^\epsilon}{\Gamma(2-\epsilon)} \int dt^2 (\vec{t}^2)^{-\epsilon} \int_0^1 d\alpha_3 B\left(\frac{\vec{q}_T^2}{m^2}, \alpha_3, t^2\right) \quad (2.23)$$

where  $B$  is related to the function  $A$  defined in Eq. (2.12) above

$$B\left(\frac{\bar{q}_T^2}{m^2}, \alpha_3, t^2\right) = \left[ NA\left(\frac{\alpha_3^2 \bar{q}_T^2}{m^2}, \alpha_3, t^2\right) - \frac{1}{2N} A\left(\frac{\bar{q}_T^2}{m^2}, \alpha_3, t^2\right) \right]. \quad (2.24)$$

We define the four dimensional impact factor  $\bar{I}$  introducing the function  $h_g$ ,

$$\bar{I}_g^{AB}(\bar{q}_T^2, m^2) = \frac{\delta^{AB} \alpha_S^2}{2V} h_g\left(\frac{\bar{q}_T^2}{m^2}\right) \quad (2.25)$$

Performing an oversubtraction about  $\bar{q}_T = 0$  we may write the full gluon impact factor as

$$\begin{aligned} I_g^{AB}(\bar{q}_T^2, m^2) &= \delta^{AB} \frac{\alpha_S^2}{2V} \left\{ \left[ h_g\left(\frac{\bar{q}_T^2}{m^2}, m^2\right) - \frac{\bar{q}_T^2}{m^2} h'_g(0) \theta(\mu^2 - \bar{q}_T^2) \right] \right. \\ &+ \left. \frac{\bar{q}_T^2}{m^2} \theta(\mu^2 - \bar{q}_T^2) \frac{(4\pi\mu^2)^\epsilon}{\Gamma(2-\epsilon)} \left(\frac{\mu^2}{m^2}\right)^\epsilon \left( N\left(\frac{4}{15} - \frac{3}{10}\epsilon\right) - \frac{1}{2N}\left(\frac{7}{9} - \frac{8}{9}\epsilon\right) + O(\epsilon^2) \right) \right\} \end{aligned} \quad (2.26)$$

The expression for the function  $h_g$  is given in Section 4. The weighted integral of  $h_g$  appropriate for the calculation of the cross section using Eq. (2.9) is given by,

$$\begin{aligned} &\int_0^\infty \frac{da}{a^2} [h_g(a) - a h'_g(0) \theta(\mu^2 - am^2)] = \\ &N \left[ \left( \frac{154}{225} - \frac{1}{2N^2} \frac{41}{27} \right) - \ln\left(\frac{\mu^2}{m^2}\right) \left( \frac{4}{15} - \frac{1}{2N^2} \frac{7}{9} \right) \right] \end{aligned} \quad (2.27)$$

Hence we obtain an expression for the unfactorised cross section for gluon quark scattering,

$$\begin{aligned} \sigma_{gq} &= \frac{\alpha_S^3}{m^2} \left\{ \left[ \left( \frac{77}{225} - \frac{1}{2N^2} \frac{41}{54} \right) - \ln\left(\frac{\mu^2}{m^2}\right) \left( \frac{2}{15} - \frac{1}{2N^2} \frac{7}{18} \right) \right] \right. \\ &+ \left. \frac{(4\pi\mu^2)^{2\epsilon}}{\Gamma(1-\epsilon)\Gamma(2-\epsilon)} \left(\frac{\mu^2}{m^2}\right)^\epsilon \int_0^{\mu^2} \frac{d\bar{q}_T^2}{(\bar{q}_T^2)^{1+\epsilon}} \left( \frac{2}{15} - \frac{3}{20}\epsilon - \frac{1}{2N^2} \left[ \frac{7}{18} - \frac{4}{9}\epsilon \right] \right) \right\} \end{aligned} \quad (2.28)$$

The factorisation piece in the  $\overline{MS}$  scheme can be derived using the  $n$  dimensional matrix elements of Table 1 and Eq. (2.18).

$$\sigma_{gq}^{AP} = \frac{\alpha_S^3}{(m^2)^{1+\epsilon}} \frac{(4\pi\mu^4)^\epsilon}{\Gamma(2-\epsilon)} \left[ -\frac{2}{15} \frac{1}{\bar{\epsilon}} + \frac{3}{20} + \frac{1}{2N^2} \left( \frac{7}{18} \frac{1}{\bar{\epsilon}} - \frac{4}{9} \right) \right] \quad (2.29)$$

Performing the factorisation by subtracting Eq. (2.29) from Eq. (2.28) the result for the gluon-quark short distance cross section is,

$$\hat{\sigma}_{gq} = \frac{\alpha_S^3}{m^2} \left[ \left( \frac{77}{225} - \frac{1}{2N^2} \frac{41}{54} \right) - \ln \left( \frac{\mu^2}{m^2} \right) \left( \frac{2}{15} - \frac{1}{2N^2} \frac{7}{18} \right) \right] \quad (2.30)$$

Taking into account that either gluon one or gluon two can act as a source for the exchanged eikonal gluon the gluon-gluon heavy quark production cross section is obtained by multiplying Eq. (2.30) by an overall factor.

$$\hat{\sigma}_{gg} = 2 \frac{2N^2}{V} \hat{\sigma}_{gq} \quad (2.31)$$

Eqs. (2.30) and (2.31) can be seen to be consistent with the results for  $f_{gg}^{(1)}$ ,  $\bar{f}_{gg}^{(1)}$  plotted in Fig. 3 in the high energy limit. The analytic results given in ref. [12] for  $\hat{\sigma}_{gq}$  and  $\hat{\sigma}_{gq}$  contain errors.

### 3. Direct Photon Production in Hadron-Hadron Scattering

The total cross section for the production of direct photons contains a mass singularity, so we consider the cross section for the production of direct photons with transverse momentum  $\vec{k}_T$  larger than some fixed value  $\vec{p}_T$ . The short distance cross section for this process is given in perturbation theory by,

$$\hat{\sigma}_{ij}(\vec{k}_T > \vec{p}_T) = \frac{\alpha\alpha_S(\mu^2)}{\vec{p}_T^2} \left\{ e_{ij}^{(0)}(\rho) + 4\pi\alpha_S \left[ e_{ij}^{(1)}(\rho) + \ln \left( \frac{\mu^2}{\vec{p}_T^2} \right) \bar{e}_{ij}^{(1)}(\rho) \right] + \dots \right\} \quad (3.1)$$

where

$$\rho = \frac{4\vec{p}_T^2}{s}, \quad \beta = \sqrt{1 - \rho}. \quad (3.2)$$

The leading order graphs for this process are shown in Fig. 6. The resultant matrix elements calculated in  $n$  dimensions are given in Table 1. From these matrix elements one may calculate the explicit expressions for  $e^{(0)}$  which are given in Table 2. In next order,  $O(\alpha\alpha_S^2)$ , the terms giving the leading power behaviour are shown in Fig. 7. The impact factor for direct photon production can be derived from the upper part of these diagrams. Defining the impact factor by Eq. (2.7) and performing the Sudakov

decomposition we obtain,

$$I_q^{AB}(\vec{q}_T^2, \vec{p}_T^2) = \delta^{AB} \frac{e_q^2 \alpha \alpha_S}{2N} \frac{\mu^{4\epsilon} \Gamma(1-\epsilon)}{\pi^{1-\epsilon} \Gamma(1-2\epsilon)} \\ \times \vec{q}_T^2 \int_0^\pi d\phi \sin^{-2\epsilon} \phi \int_0^1 d\alpha_3 \int_{\vec{p}_T^2}^\infty dt^2 (\vec{t}^2)^{-\epsilon} C(\vec{q}_T, \alpha_3, \vec{t}) \quad (3.3)$$

where

$$C(\vec{q}_T, \alpha_3, \vec{t}) = \frac{4\alpha_3(1-\alpha_3) + 2\alpha_3^3(1-\epsilon)}{\vec{t}^2(\vec{t} - \alpha_3 \vec{q}_T)^2} \quad (3.4)$$

and  $\phi$  is the angle between  $\vec{q}_T$  and  $\vec{t}$ . As in the previous section it is convenient to define the four-dimensional impact factor  $\bar{I}_q$ ,

$$\bar{I}_q^{AB}(\vec{q}_T^2, \vec{p}_T^2) = \delta^{AB} \frac{e_q^2 \alpha \alpha_S}{2N} h_q\left(\frac{\vec{q}_T^2}{\vec{p}_T^2}\right) \quad (3.5)$$

The impact factor oversubtracted about the point  $\vec{q}_T = 0$  is,

$$I_q^{AB}(\vec{q}_T^2, \vec{p}_T^2) = \delta^{AB} \frac{e_q^2 \alpha \alpha_S}{2N} \left\{ \left[ h_q\left(\frac{\vec{q}_T^2}{\vec{p}_T^2}\right) - \frac{\vec{q}_T^2}{\vec{p}_T^2} h'_q(0) \theta(\mu^2 - \vec{q}_T^2) \right] \right. \\ \left. + \frac{\vec{q}_T^2}{\vec{p}_T^2} \theta(\mu^2 - \vec{q}_T^2) \frac{(4\pi\mu^2)^\epsilon}{\Gamma(1-\epsilon)} \left(\frac{\mu^2}{\vec{p}_T^2}\right)^\epsilon \left(\frac{7}{6} - \frac{5}{3}\epsilon + O(\epsilon^2)\right) \right\} \quad (3.6)$$

The integrals in Eq. (3.3) can be performed explicitly in four dimensions to give the following result for the function  $h_q(a)$ ,

$$h_q(a) = \left[ \left( \frac{3}{2} + \frac{1}{2a} - \ln a \right) \ln(1-a)^2 + \frac{\pi^2}{3} - 2 \text{Li}_2(1-a) - 7 + \frac{2}{\sqrt{a}} \ln \left( \frac{1 + \sqrt{a}}{1 - \sqrt{a}} \right)^2 \right] \quad (3.7)$$

The function  $h_q$  vanishes in the small  $a$  region,

$$h_q(a) = \frac{7a}{6} + O(a^2) \quad (3.8)$$

The necessary weighted integral of this function, subtracted at  $\vec{q}_T = 0$  is given by,

$$\int_0^\infty \frac{da}{a^2} \left[ h_q(a) - a h'_q(0) \theta(\mu^2 - a\vec{p}_T^2) \right] = \frac{91}{36} - \frac{7}{6} \ln \frac{\mu^2}{\vec{p}_T^2} \quad (3.9)$$

Once again the cross section can be written as

$$\sigma_{qj} = \pi \frac{(4\pi)^\epsilon}{\Gamma(1-\epsilon)} \int \frac{d\vec{q}_T^2}{(\vec{q}_T^2)^{2+\epsilon}} \left[ \sum_{A,B} I_q^{AB} K_j^{AB} \right] + O\left(\frac{1}{s}\right) \quad (3.10)$$

where  $K_j^{AB}$  is given by Eq. (2.10) and  $I_q^{AB}$  is given by Eq. (3.6). The final result for the unfactorised cross section is therefore given by

$$\begin{aligned} \sigma_{qg}(\vec{k}_T > \vec{p}_T) &= \frac{e_q^2 \alpha \alpha_S^2}{\vec{p}_T^2} \left\{ \left[ \frac{91}{36} - \frac{7}{6} \ln \frac{\mu^2}{\vec{p}_T^2} \right] \right. \\ &\quad \left. + \frac{(4\pi\mu^2)^{2\epsilon}}{\Gamma(1-\epsilon)\Gamma(1-\epsilon)} \left( \frac{\mu^2}{\vec{p}_T^2} \right)^\epsilon \int_0^{\mu^2} \frac{d\vec{q}_T^2}{(\vec{q}_T^2)^{1+\epsilon}} \left( \frac{7}{6} - \frac{5}{3}\epsilon \right) \right\} \quad (3.11) \end{aligned}$$

In contrast to the processes in Section 2, these graphs have two sources of collinear divergences. One is the above-mentioned case where the exchanged gluon goes on mass shell and is removed by subtracting the Altarelli-Parisi function for a gluon emitted from a gluon convoluted with the leading order cross section derived from the graphs shown in Fig. 6b. The other divergence arises when the direct photon is collinear with the emerging quark and is present in the graph of Fig. 7b in a physical gauge. This divergence must be absorbed into the fragmentation function of the outgoing quark and is removed by subtracting the Altarelli-Parisi function for the emission of a photon from a quark  $P_{\gamma q}$  convoluted with the cross section for gluon-quark scattering.

$$P_{\gamma q}(z) = e_q^2 \left[ \frac{1 + (1-z)^2}{z} \right] \quad (3.12)$$

Retaining only the leading power terms we obtain the following relation between perturbative and short distance cross section,

$$\frac{E_3 d\sigma_{qg}^\gamma}{d^{n-1}p_3} = -\frac{1}{\bar{\epsilon}} \frac{\alpha_S}{2\pi} \left\{ \int \frac{dx_3}{x_3^2} P_{\gamma q}(x_3) \frac{\hat{E} d\hat{\sigma}_{qg}^q(p_3 = \hat{p}_3/x_3)}{d^{n-1}\hat{p}_3} + \int dx_2 \frac{\hat{E} d\hat{\sigma}_{qg}^\gamma(p_2 = x_2\hat{p}_2)}{d^{n-1}\hat{p}_3} P_{gq}(x_2) \right\} \quad (3.13)$$

Using the matrix elements squared given in Table 1, we find that the factorisation pieces corresponding to the two terms in Eq. (3.13) are,

$$\sigma_{qg}^{\text{AP}}(\vec{k}_T > \vec{p}_T) = \frac{e_q^2 \alpha \alpha_S^2}{(\vec{p}_T^2)^{1+\epsilon}} \frac{(4\pi\mu^4)^\epsilon}{\Gamma(1-\epsilon)} \left\{ \left( -\frac{1}{\bar{\epsilon}} \frac{7}{12} + \frac{91}{72} \right) + \left( -\frac{1}{\bar{\epsilon}} \frac{7}{12} + \frac{5}{6} \right) \right\} \quad (3.14)$$

Subtracting Eq. (3.14) from Eq. (3.11) we obtain the final result for the short distance cross section.

$$\hat{\sigma}_{qg}(\vec{k}_T > \vec{p}_T) = \frac{e_q^2 \alpha \alpha_S^2}{\vec{p}_T^2} \left[ \frac{151}{72} - \frac{7}{6} \ln \frac{\mu^2}{\vec{p}_T^2} \right] \quad (3.15)$$

This formula allows us to extract the coefficients  $e_{qg}^{(1)}(\rho)$  and  $\bar{e}_{qg}^{(1)}(\rho)$ , defined in Eq. (3.1), in the limit  $\rho \rightarrow 0$ . The results are

$$e_{qg}^{(1)}(\rho) \rightarrow \frac{151}{288\pi} e_q^2, \quad \bar{e}_{qg}^{(1)}(\rho) \rightarrow -\frac{7}{24\pi} e_q^2 \quad (3.16)$$

The complete form of the functions  $e_{qg}(\rho)$  for all values of  $\rho$  is shown in Fig. 8. This figure is obtained by numerical integration of the results of Aurenche *et al.*[13]. The high energy behaviour shown in Fig. 8 is in agreement with Eq. (3.16).

#### 4. Impact factors in four dimensions

In this section we present a series of results on the impact factors in four dimensions. The impact factor of the photon in four dimensions is obtained from Eq. (2.11) after performing two simple integrations. The result is

$$\bar{I}_\gamma^{AB}(\bar{q}_T^2, m^2) = \frac{e_Q^2 \alpha \alpha_S}{2} \delta^{AB} h_\gamma\left(\frac{\bar{q}_T^2}{m^2}\right) \quad (4.1)$$

where

$$h_\gamma(a) = \frac{2a}{3} \int_0^1 dx \frac{1+x(1-x)}{[1+x(1-x)a]}. \quad (4.2)$$

Eq. (4.2) is in agreement with the results of ref. [9]. After integration over the Feynman parameter  $x$ , the impact factor of the photon in heavy quark production can be written as,

$$h_\gamma\left(\frac{\bar{q}_T^2}{m^2}\right) = \frac{2}{3} \left[ \frac{\bar{q}_T^2 - m^2}{m^2} F\left(\frac{4m^2}{\bar{q}_T^2}\right) + 1 \right]. \quad (4.3)$$

The function  $F$  is defined as

$$F(\rho) = \int_0^1 dx \frac{\rho}{\rho + 4x(1-x)} = \frac{\rho}{2\sqrt{1+\rho}} \ln \left( \frac{\sqrt{1+\rho} + 1}{\sqrt{1+\rho} - 1} \right). \quad (4.4)$$

The power series expansion of  $F$  for large and small  $\rho$  is,

$$\begin{aligned} F(\rho) &\rightarrow 1 - \frac{2}{3\rho} + \frac{8}{15\rho^2} - \frac{16}{35\rho^3} + O(1/\rho^4) \\ F(\rho) &\rightarrow -\frac{\rho}{2} \ln\left(\frac{\rho}{4}\right) + O(\rho^2) \end{aligned} \quad (4.5)$$

The result in four dimensions for the impact factor of the gluon can be obtained from Eq. (2.23). Introducing the function  $h_g$  we find,

$$\bar{I}_g^{AB}(\bar{q}_T^2, m^2) = \frac{\alpha_s^2}{2V} \delta^{AB} h_g\left(\frac{\bar{q}_T^2}{m^2}\right) \quad (4.6)$$

where

$$h_g\left(\frac{\bar{q}_T^2}{m^2}\right) = \left[ N \int_0^1 dx \int_0^1 da_3 \frac{a_3^2 \bar{q}_T^2 [1 - 2a_3(1 - a_3)(1 - 2x(1 - x))]}{[m^2 + a_3^2 x(1 - x) \bar{q}_T^2]} - \frac{1}{2N} \frac{2\bar{q}_T^2}{3} \int_0^1 dx \frac{1 + x(1 - x)}{[m^2 + x(1 - x) \bar{q}_T^2]} \right]. \quad (4.7)$$

After integration  $h_g$  may also be written in terms of the function  $F$  defined in Eq. (4.4),

$$h_g(a) = \frac{2}{3} \left\{ N \left[ \frac{(a-2)(a+4)}{a} F\left(\frac{4}{a}\right) + \frac{8}{a} - \frac{10}{3} \right] - \frac{1}{2N} \left[ (a-1) F\left(\frac{4}{a}\right) + 1 \right] \right\} \quad (4.8)$$

In the limit of small argument  $a$  we obtain for these impact factors,

$$\begin{aligned} h_\gamma(a) &= \frac{7}{9}a + O(a^2) \\ h_g(a) &= \left[ \frac{4N}{15} - \frac{1}{2N} \frac{7}{9} \right] a + O(a^2). \end{aligned} \quad (4.9)$$

It is also useful to introduce the scaled impact factor which is defined as follows

$$j_k(a) = \frac{h_k(a)}{a}, \quad \text{for } k = \gamma, g, q. \quad (4.10)$$

A plot of the scaled impact factors is shown in Fig. 9. At low  $\bar{q}_T$  the plots exhibit a plateau as determined by Eqs. (3.8, 4.9). This is expected from the discussion of ref. [14]. The fact that the functions  $h$  vanish linearly for small  $a$  can also be understood physically. A low momentum gluon cannot resolve the various coloured constituents of the upper blob. When the momentum  $q_T$  becomes larger than the characteristic momentum in the upper blob, the participating partons are resolved and the cancellation between different diagrams no longer occurs. Consequently at higher values of  $\bar{q}_T$  the scaled impact factors  $j_k$  make a transition to a  $1/a$  behaviour (modulo logarithms). We may estimate the position of this transition by choosing the point at which the scaled impact factor  $j_k$  has dropped to half of its plateau value.

$$j_\gamma(6.65) = \frac{1}{2} j_\gamma(0), \quad |\bar{q}_T| = 2.6m$$

$$\begin{aligned}
j_g(13.5) &= \frac{1}{2}j_g(0), & |\vec{q}_T| &= 3.7m \\
j_q(4.75) &= \frac{1}{2}j_q(0), & |\vec{q}_T| &= 2.2|\vec{p}_T|
\end{aligned}
\tag{4.11}$$

Therefore the scale at which the cancellation between different diagrams ceases to occur because of the injection of an appreciable momentum into the upper part of the graph is a few times the mass or  $\vec{p}_T$ .

An issue of importance in heavy quark production is the relative magnitude of the gluon fragmentation contributions (such as the gluon splitting diagram shown in last graph of Fig. 5b) and the flavour creation diagrams. We define the flavour creation diagrams to be the diagrams shown in Fig. 1a dressed with final and initial state gluon bremsstrahlung. The distinction between the two types of diagrams has meaning only in the leading logarithm approximation. Let us introduce the oversubtracted impact factor,  $\mathcal{H}$ ,

$$\mathcal{H}(q_T^2, m^2, \mu^2) = \left[ h_g\left(\frac{q_T^2}{m^2}\right) - \theta(\mu^2 - q_T^2) \frac{q_T^2}{m^2} h'_g(0) \right]
\tag{4.12}$$

where  $h'_g$  denotes the derivative as before. Eq. (4.12) can be used to calculate the net contribution of the higher order diagrams shown in Fig. 5b, after factorisation in the  $\overline{MS}$  scheme. This estimate is valid only in the high energy limit. The integral of  $\mathcal{H}$  which is relevant for the calculation of the total cross-section in gluon-gluon fusion is given in Eq. (2.27).

In a Monte-Carlo program one attempts to give an exclusive description of a hard scattering event. After integration over all other momenta the Monte-Carlo programs should yield a result for the total cross section which agrees with the exact result in the leading logarithmic approximation. In practice this means that the function  $\mathcal{H}$  is approximated by a function  $\mathcal{H}^{\text{MC}}$  which correctly reproduces only the leading logarithmic pieces. The hard scattering of two gluons is included in a Monte-Carlo program with some cut-off on the transverse momentum  $\vec{q}_T^2 > \mu_0^2$ . As a model of the logarithmic terms included in a Monte-Carlo program in the high energy limit, we shall take

$$\mathcal{H}^{\text{MC}}(q_T^2, m^2, \mu^2) = \theta(\vec{q}_T^2 - \mu_0^2) \frac{4N^2 - 2}{3N} \log\left(\frac{\vec{q}_T^2}{4m^2}\right).
\tag{4.13}$$

The exact choice of the constant term present in the argument of the logarithm in Eq. (4.13) is undetermined in the leading logarithmic approximation. It is a matter of some delicacy since the Monte-Carlo programs are often used in a region in which the logarithms are not large enough to dominate numerically. In practice the particular

constant terms which are included will vary between Monte-Carlo programs. The choice of  $\mu$  and  $\mu_0$  can be made independently in the Eqs. (4.12,4.13), subject to the constraint that they should lead the same total cross-section. In practice there are conflicting requirements on the choice of  $\mu$  and  $\mu_0$ . In the exact expression, Eq. (4.12), we wish to choose  $\mu$  to be small so that most of the physics of gluon radiation is described by the higher order matrix element rather than being incorporated into the structure function. In the Monte-Carlo function, Eq. (4.13), we wish to keep the scale  $\mu_0$  large so that the leading logarithmic approximation is warranted. As a compromise solution we choose  $\mu^2 = 4.33m^2$  in Eq.(4.12) and  $\mu_0^2 = 4m^2$  in the approximate formula, Eq.(4.13). Other choices are clearly possible, but in this case both curves integrate to give the same total cross section. Using these choices for  $\mu$  and  $\mu_0$ , the scaled impact factors are shown plotted in Fig. 10. Note also that because of the astute choice for the constant piece in Eq. (4.13), the two curves coincide well for  $\bar{q}_T^2 > 10m^2$ . It would be interesting to try and apply this matching procedure to a realistic Monte-Carlo program.

## 5. Conclusions

We have considered the leading power corrections to three hard scattering processes. The conclusions for the total cross sections are summarised in Table 3, which reports the numerical values of the terms which govern the asymptotic behaviour, as well as the choice of  $\mu$  which leads to a cancellation of the leading high energy behaviour. A possible conclusion from these results is that the most appropriate choice for  $\mu$  is given by  $\mu = km$  or  $\mu = k|\vec{p}_T|$  where  $k$  is between 2.5 and 4. With a choice of  $k$  in this range the effect of higher order terms in the cross section is reduced. The amount of reduction can be calculated from Table 3. As a by-product of this investigation we have shown that the subtraction scale in the  $\overline{MS}$  scheme has a direct physical interpretation, because the values of  $\mu$  in Table 3 and in Eq. (4.11) are approximately in agreement. The disadvantage of choosing the scale to minimise the high energy correction is apparent from Figs. 2, 3 and 8, where it is shown that this choice increases the size of the radiative corrections near threshold.

We therefore tentatively propose another possibility. Consider a process with a single incoming line  $i$ . The perturbatively calculated cross section  $\sigma$  and the short

distance cross section  $\hat{\sigma}$  are related by

$$\sigma_i = \hat{\sigma}_j \otimes \Gamma_{ji}(x, \epsilon) \quad (5.1)$$

The symbol  $\otimes$  indicates the normal convolution. Some of the leading power correction to the processes considered above can be removed by modifying the factorisation pieces  $\Gamma$  on the incoming lines as follows,

$$\begin{aligned} \Gamma_{qq}(x, \epsilon) &= \delta(1-x) - \frac{\alpha_S}{2\pi} \left(\frac{1}{\bar{\epsilon}}\right) P_{qq}(x) \\ \Gamma_{qg}(x, \epsilon) &= -\frac{\alpha_S}{2\pi} \left(\frac{1}{\bar{\epsilon}}\right) P_{qg}(x) \\ \Gamma_{gq}(x, \epsilon) &= -\frac{\alpha_S}{2\pi} \left(\frac{1}{\bar{\epsilon}} P_{gq}(x) - k \frac{V}{Nx}\right) \\ \Gamma_{gg}(x, \epsilon) &= \delta(1-x) - \frac{\alpha_S}{2\pi} \left(\frac{1}{\bar{\epsilon}} P_{gg}(x) - k \frac{2N}{x}\right) \end{aligned} \quad (5.2)$$

where  $P$  are the standard one loop Altarelli-Parisi functions and

$$\frac{1}{\bar{\epsilon}} = \frac{1}{\epsilon} + \ln 4\pi - \gamma_E \quad (5.3)$$

The subtractions  $\Gamma_{qq}$  and  $\Gamma_{qg}$  are those of the standard  $\overline{MS}$  scheme, but the subtractions  $\Gamma_{gq}$  and  $\Gamma_{gg}$  are new. This is a further modification of the modified minimal subtraction scheme, but it will have little effect on most phenomenology, because few precision experiments are sensitive to the gluon distribution function. A suitable value for the constant  $k$  is 2.53. In the initial state factorisation scheme defined by this value of  $k$  we obtain

$$\begin{aligned} c_{\gamma_g}^{(1)} &\rightarrow -0.108 \\ f_{gg}^{(1)} &\rightarrow 0.006 \\ e_{gg}^{(1)} &\rightarrow 0.049 \end{aligned} \quad (5.4)$$

This leads to a reduction of the coupling to the QCD pomeron of at least a factor of 3.4. This will be accompanied by a change in the higher order corrections to the gluon structure function as determined in Deep Inelastic Scattering. The effect of our proposed renormalisation scheme is to move the major part of the QCD pomeron

into the low  $x$  behaviour of the gluon distribution, which is common to all semi-hard processes.

In conclusion, we see that for several cases in which the pomeron couples to hard scattering processes at next to leading order, the large power enhanced correction may be removed by an appropriate choice of scale. This choice makes sense physically at high energy, but it increases the size of the corrections in the region near threshold. A second method is to factorise the correction into the low  $x$  behaviour of the gluon distribution function. This modification of the factorisation prescription changes the anomalous dimension at two loops. For gluon distribution functions compared at approximately the same values of  $\mu^2$ , this modification of the evolution properties will have little significance.

## Acknowledgement.

We would like to acknowledge useful discussions with P. Aurenche and J. C. Collins. This work was initiated at the Institute for Theoretical Physics of the University of Santa Barbara and we express our gratitude for the hospitality of the institute. The research was supported in part by the National Science foundation under grant No. PHY82-17853, supplemented by funds from the National Aeronautics and Space Administration.

## Appendix A: Results for four quark production

In this appendix we present a series of results on the high energy limit of the cross section for the production of two pairs of heavy quarks.

$$i + j \rightarrow Q + \bar{Q} + Q + \bar{Q}. \quad (\text{A.1})$$

In terms of the impact factors this cross section is given by,

$$\sigma_{ij} = \frac{1}{\pi} \int \frac{d\bar{q}_T^2}{\bar{q}_T^4} \left[ \sum_{A,B} \bar{I}_i^{AB}(\bar{q}_T^2, m^2) \bar{I}_j^{AB}(\bar{q}_T^2, m^2) \right] + O\left(\frac{1}{s}\right) \quad (\text{A.2})$$

In the asymptotic region the  $\bar{q}_T^2$  integral can be taken to extend from zero to infinity. Inserting the expressions for the impact factors given in Eqs. (4.3) and (4.8) and

performing the integrals the result for the reaction  $\gamma\gamma \rightarrow Q\bar{Q}Q\bar{Q}$  at high energy is in agreement with ref. [9].

$$\sigma_{\gamma\gamma} = \frac{\alpha_S^2 e_Q^4 \alpha^2}{\pi m^2} k_{\gamma\gamma}, \quad k_{\gamma\gamma} = V \left[ \frac{175}{144} \zeta(3) - \frac{19}{72} \right] \approx 9.58 \quad (\text{A.3})$$

where  $\zeta(3) = 1.2021$ . For heavy quark production by photon gluon fusion,  $\gamma g \rightarrow Q\bar{Q}Q\bar{Q}$ , the result is,

$$\sigma_{\gamma g} = \frac{\alpha_S^3 e_Q^2 \alpha}{\pi m^2} k_{\gamma g}, \quad k_{\gamma g} = \left[ \frac{277N}{486} + \frac{19}{144N} - \frac{175}{288N} \zeta(3) \right] \approx 1.51 \quad (\text{A.4})$$

Lastly we give the result for gluon-gluon fusion,  $gg \rightarrow Q\bar{Q}Q\bar{Q}$ ,

$$\sigma_{gg} = \frac{\alpha_S^4}{\pi m^2} k_{gg}, \quad k_{gg} = \frac{1}{V} \left[ \frac{175}{576N^2} \zeta(3) + \frac{23N^2}{81} - \frac{277}{486} - \frac{19}{288N^2} \right] \approx 0.252 \quad (\text{A.5})$$

Eq. (A.5) may be useful in estimating the backgrounds to  $B - \bar{B}$  mixing.

## References

- 1) L. V. Gribov, E. M. Levin and M. G. Ryskin, *Phys. Rep.* **100** (1983) 1 .
- 2) L. N. Lipatov in "Perturbative QCD", World Scientific (1989), A. H. Mueller, (editor).
- 3) A. H. Mueller and H. Navelet, *Nucl. Phys.* **B282** (1987) 727 .
- 4) See, for example, R. K. Ellis, Proceedings of the 1987 Theoretical Advanced Study Institute, (R. Slansky and G. West, Editors).
- 5) W. A. Bardeen *et al.*, *Phys. Rev.* **D18** (1978) 3998 .
- 6) G. Altarelli and G. Parisi, *Nucl. Phys.* **B126** (1977) 298 .
- 7) R. K. Ellis and P. Nason, *Nucl. Phys.* **B312** (1989) 551 .
- 8) P. Nason, S. Dawson and R. K. Ellis, *Nucl. Phys.* **B303** (1988) 607 .

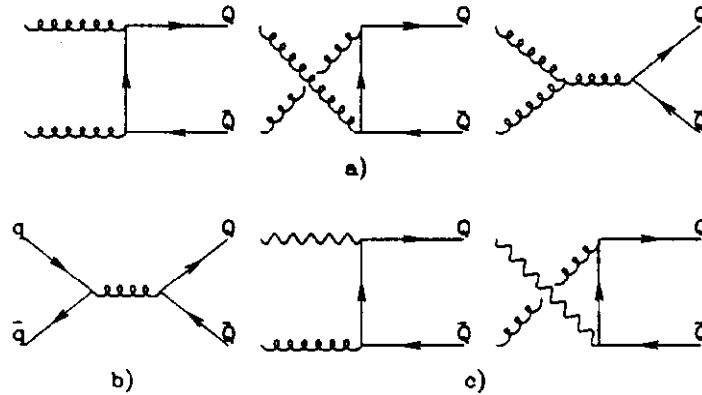


Figure 1: Lowest order diagrams for heavy quark production by hadrons (a,b) and by photons (c).

- 9) L. N. Lipatov and G. V. Frolov, *Sov. J. Nucl. Phys.* **13** (1971) 333 .
- 10) Ya. Ya. Balitskii and L. N. Lipatov, *Sov. J. Nucl. Phys.* **28** (1978) 822 .
- 11) H. Cheng and T. T. Wu, *Phys. Rev.* **182** (1969) 1852,1868,1873,1899 .
- 12) R. K. Ellis, Proc. of the Workshop on QCD hard hadronic processes, St. Croix, Virgin Islands, (1987).
- 13) P. Aurenche *et al.*, *Nucl. Phys.* **B297** (1988) 661 .
- 14) J. C. Collins, D. E. Soper and G. Sterman, *Nucl. Phys.* **B263** (1986) 37 .

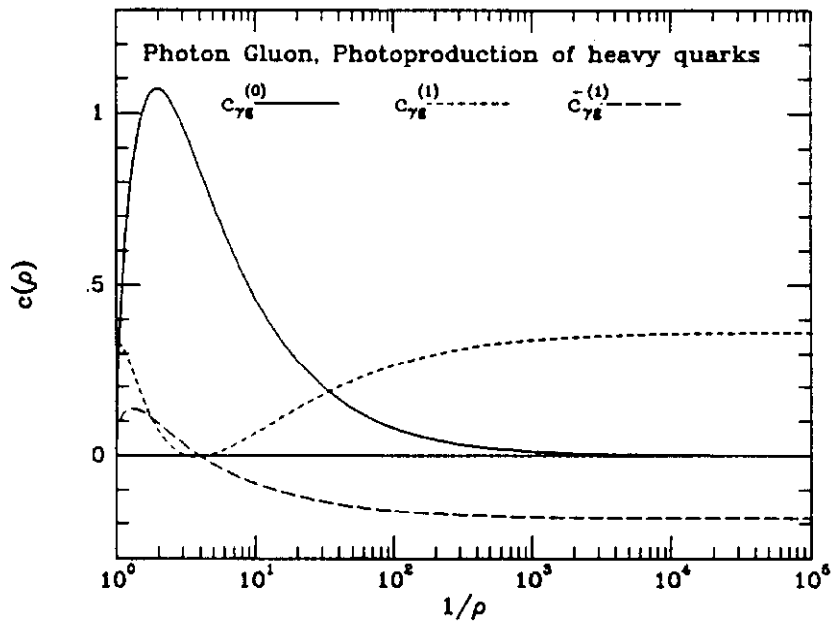


Figure 2: Photon-gluon coefficients defined by Eq. (2.1)

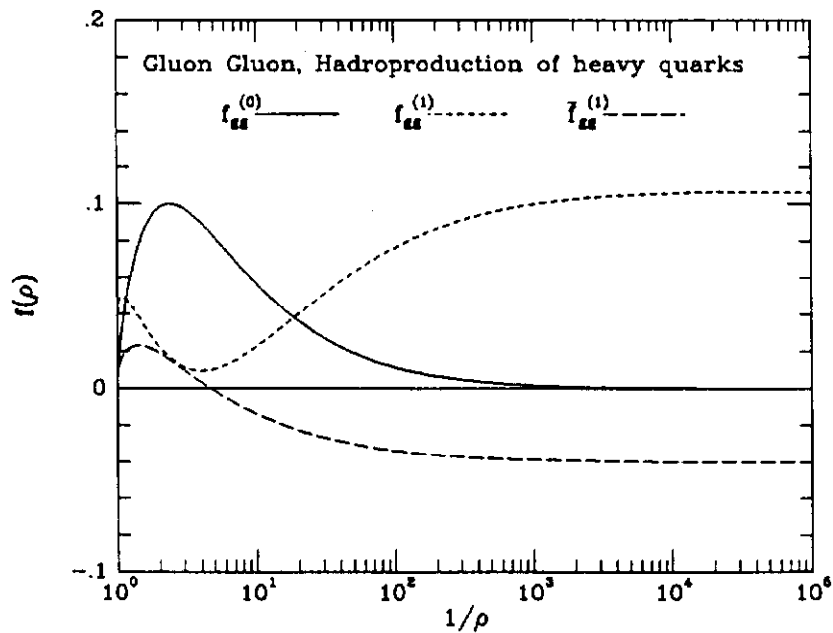


Figure 3: Gluon-gluon coefficients defined by Eq. (2.2)

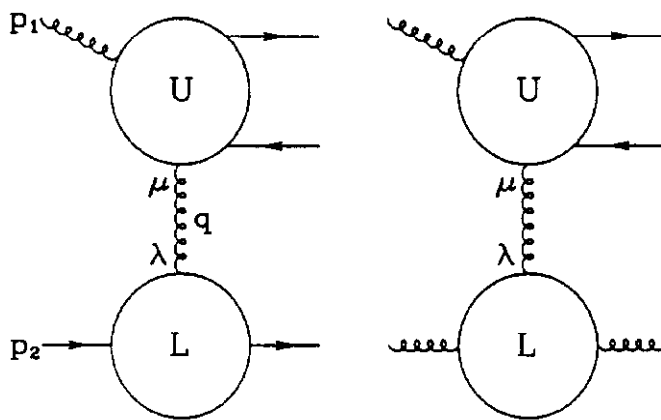


Figure 4: Diagrams with spin one exchange.

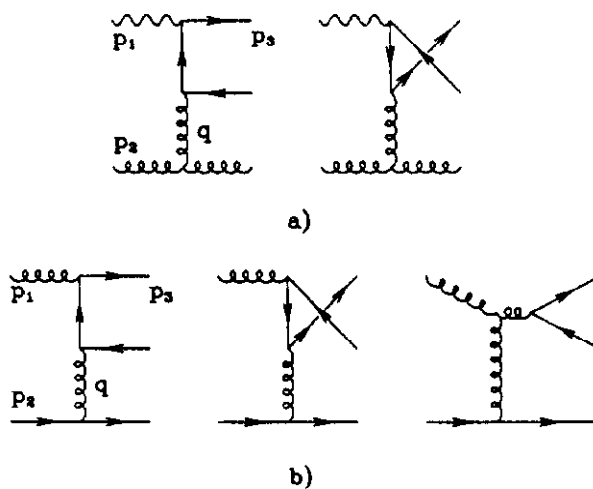


Figure 5: Diagrams for heavy quark production with spin one exchange.

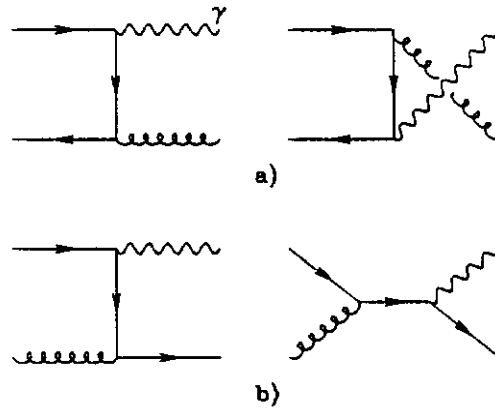


Figure 6: Lowest order diagrams for direct photon production.

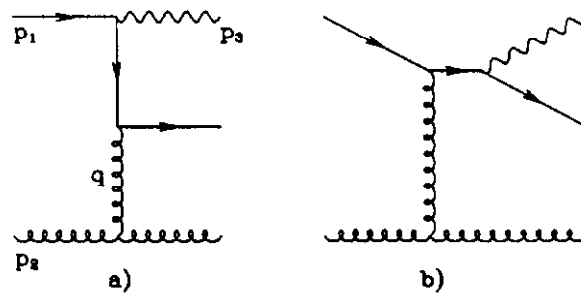


Figure 7: Diagrams for direct photon production with spin one exchange.

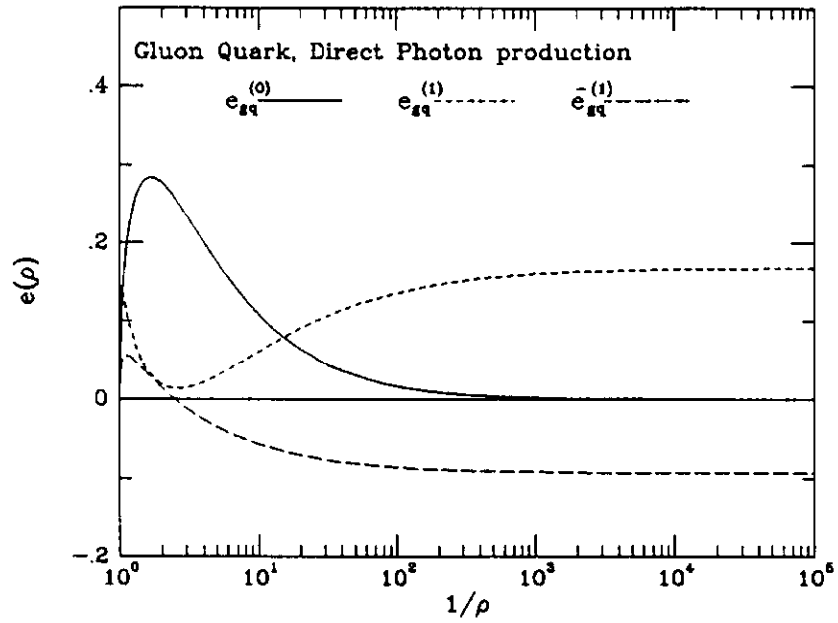


Figure 8: Plot of direct photon production cross-section

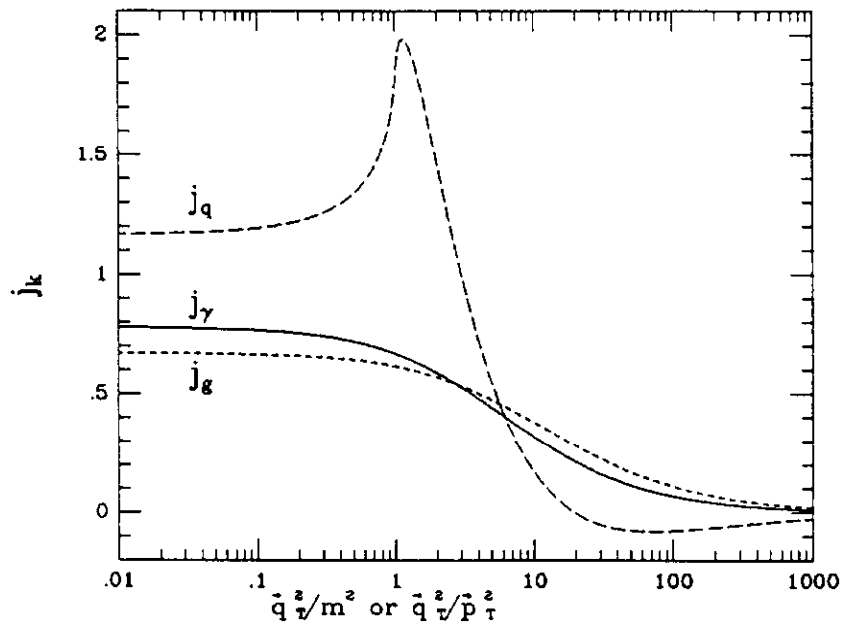


Figure 9: Scaled impact factors  $j_k$

Process $p_1 + p_2 \rightarrow p_3 + p_4$	$\sum  M ^2$
$q + \bar{q} \rightarrow Q + \bar{Q}$	$\frac{g^4 V}{2N^2} (\tau_1^2 + \tau_2^2 + \frac{\rho}{2} - \epsilon)$
$g + g \rightarrow Q + \bar{Q}$	$\frac{g^4 (V - 2N^2 \tau_1 \tau_2)}{2VN(1 - \epsilon)^2 \tau_1 \tau_2} \left( (1 - \epsilon)(\tau_1^2 + \tau_2^2 - \epsilon) + \rho - \frac{\rho^2}{4\tau_1 \tau_2} \right)$
$\gamma + g \rightarrow Q + \bar{Q}$	$\frac{e^2 e_Q^2 g^2}{(1 - \epsilon)^2 \tau_1 \tau_2} \left( (1 - \epsilon)(\tau_1^2 + \tau_2^2 - \epsilon) + \rho - \frac{\rho^2}{4\tau_1 \tau_2} \right)$
$q + g \rightarrow \gamma + q$	$\frac{e^2 e_q^2 g^2}{N} \left( \frac{1 + \tau_1^2 - \epsilon \tau_2^2}{\tau_1} \right)$
$q + \bar{q} \rightarrow \gamma + g$	$\frac{e^2 e_q^2 g^2 V (1 - \epsilon)}{N^2} \left( \frac{\tau_1^2 + \tau_2^2 - \epsilon}{\tau_1 \tau_2} \right)$

Table 1: Lowest order processes in n dimensions.

Process	$\sigma_{ij}$
$c_{\gamma g}^{(0)}(\rho)$	$\frac{\pi\beta\rho}{4}[(3 - \beta^4)\mathcal{F}(\beta) - 4 + 2\beta^2]$
$f_{q\bar{q}}^{(0)}(\rho)$	$\frac{V\pi\beta\rho}{24N^2}[(2 + \rho)]$
$f_{gg}^{(0)}(\rho)$	$\frac{\pi\beta\rho}{24VN}[3[\rho^2 + 2V(\rho + 1)]\mathcal{F}(\beta) - 4 - 5\rho - V(10 + 11\rho)]$
$e_{q\bar{q}}^{(0)}(\rho)$	$\frac{V\pi\rho\beta}{2N^2}[\mathcal{F}(\beta) - 1], \mathcal{F}(\beta) = \frac{1}{\beta} \ln\left(\frac{1+\beta}{1-\beta}\right)$
$e_{gq}^{(0)}(\rho)$	$\frac{\pi\rho\beta}{8N}[2\mathcal{F}(\beta) + 1]$

Table 2: Cross sections for lowest order processes with  $\beta = \sqrt{1 - \rho}$ .

Process	$x_{ij}^{(1)}$	$\bar{x}_{ij}^{(1)}$	$x_{ij}^{(1)}/\bar{x}_{ij}^{(1)}$	$\mu$ choice
$c_{\gamma g}^{(1)} : \gamma g \rightarrow Q\bar{Q} + X$	0.363	-0.186	-1.95	$\mu = 2.65m$
$f_{gg}^{(1)} : gg \rightarrow Q\bar{Q} + X$	0.107	-0.040	-2.69	$\mu = 3.83m$
$e_{gq}^{(1)} : qg \rightarrow \gamma q + X$	0.1669	-0.0928	-1.80	$\mu = 2.46 \vec{p}_T $

Table 3: High energy behaviour of hard scattering cross-sections as defined in Eqs. 2.1, 2.2 and 3.1.

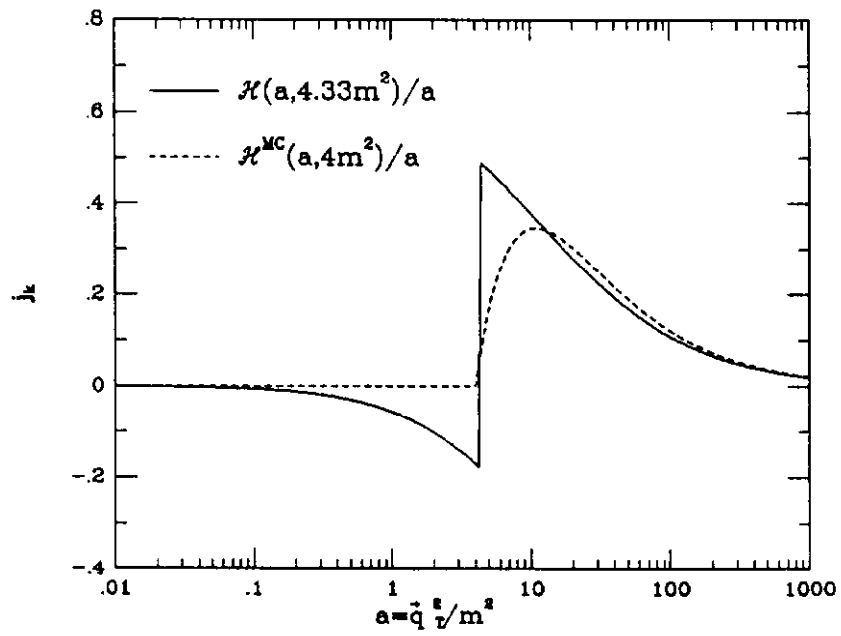


Figure 10: Subtracted and scaled impact factor for heavy quark production